Effect of confinement on flexural ductility design of concrete beams

X.C. Chen[1,2a], Z.Z. Bai[*1] and F.T.K. Au[3b]

[1]*Department of Bridge Engineering, Tongji University, Shanghai, P.R. China*
[2]*Research and Technology Center, Shenzhen WISE-TECH Engineering Consulting Co. LTD. , Shenzhen, China*
[3]*Department of Civil Engineering, The University of Hong Kong, Pokfulam Road, Hong Kong, P.R. China*

Abstract.   Seismic design of reinforced concrete (RC) structures requires a certain minimum level of flexural ductility. For example, Eurocode EN1998-1 directly specifies a minimum flexural ductility for RC beams, while Chinese code GB50011 limits the equivalent rectangular stress block depth ratio at peak resisting moment to achieve a certain nominal minimum flexural ductility indirectly. Although confinement is effective in improving the ductility of RC beams, most design codes do not provide any guidelines due to the lack of a suitable theory. In this study, the confinement for desirable flexural ductility performance of both normal- and high-strength concrete beams is evaluated based on a rigorous full-range moment-curvature analysis. An effective strategy is proposed for flexural ductility design of RC beams taking into account confinement. The key parameters considered include the maximum difference of tension and compression reinforcement ratios, and maximum neutral axis depth ratio at peak resisting moment. Empirical formulae and tables are then developed to provide guidelines accordingly.

Keywords: confinement; curvature ductility factor; flexural ductility design; RC beams; reinforcement ratios; neutral axis depth ratio

1. Introduction

For the safety of reinforced concrete (RC) structures under earthquake, both strength and ductility are important. The plastic hinges of RC beams and columns that possess high flexural ductility can absorb excessive energy through inelastic deformation before the resisting moment drops significantly thereby boosting the chance of survival of the structure. Therefore, proper flexural ductility design is important to RC members in buildings designed to withstand earthquakes. It is especially crucial for high-strength concrete (ACI Committee 363, 1992) that is inherently more brittle than normal-strength concrete.

Existing seismic or non-seismic design codes already require control of flexural ductility for RC beams. Clause 6.3.3 of Chinese code GB50011-2010 (Ministry of Construction of the People's Republic of China, 2010) effectively limits the equivalent rectangular stress block depth ratio to 0.25 and 0.35 for seismic resistance Categories I and II respectively. Clause 5.2.3.4(2) of Eurocode BS EN 1998-1:2004 (European Committee for Standardisation, 2004a) requires that sufficient curvature ductility should be provided in all local critical regions for primary seismic elements. Clause 5.2.3.4(3) of Eurocode EN 1998-1:2004 further specifies the minimum curvature ductility factor μ_{min}, the value of which is related to the basic value of behaviour factor depending on the type of

structural system. Clause 9.3.3 of American Code ACI 318-14 (ACI Committee 318, 2014) limits the minimum tension steel strain at peak resisting moment to 0.004, so that sufficient flexural ductility can be provided. Moreover, ACI 318-14 also limits the maximum reinforcement ratio in beam sections to 2.5% for special moment resisting frames.

A few researchers have worked on the flexural ductility performance of RC components. Pandey (2013) investigated the effect of high strain rate on the flexural ductility of rectangular beams; Baji and Ronagh (2014) investigated the reliability of minimum flexural ductility of the current design codes made with normal strength concrete; Chen and Ho (2015) worked on the effect of strain gradient on flexural ductility of RC columns; while Komleh and Maghsoudi (2015) investigated flexural ductility of fiber reinforced polymer (FRP) beams. Moreover, a numerical method has been developed for full-range moment-curvature analysis of RC beams extended well into the post-peak range under monotonic or cyclic loading, and applied to rectangular RC beams (Pam *et al.* 2001, Kwan *et al.* 2004, Ho *et al.* 2005, Bai *et al.* 2007, Lee 2013) and flange beams (Au and Kwan 2004, Kwan and Au 2004).

The method has also been extended to prestressed concrete beams with corrugated steel webs (Chen *et al.* 2015) and RC columns (Au and Bai 2006, Bai and Au 2009). A general strategy for flexural ductility design of concrete beams and columns has recently been proposed by Bai and Au (2013a, b) and Bai *et al.* (2015).

As observed in the tests of various investigators (Priastiwi *et al.* 2014, Ziara *et al.* 1995), confinement is effective in improving ductility but most design codes do not provide any guidelines for using confinement for the flexural ductility design of RC beams. In this study, the

---

∗Corresponding author, Ph.D.
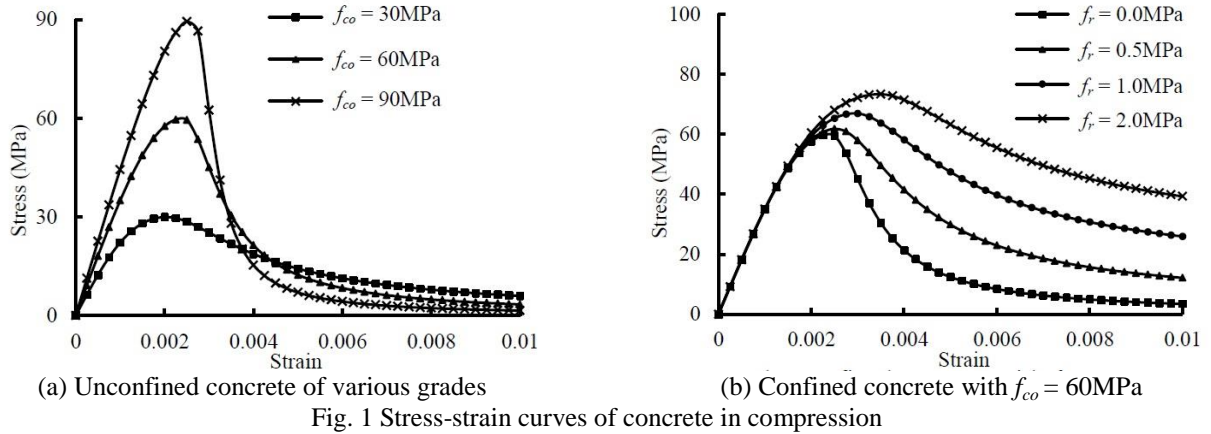 E-mail: zzbai@tongji.edu.cn
[a]Ph.D.
[b]Professor.

(a) Unconfined concrete of various grades   (b) Confined concrete with f_{co} = 60MPa

Fig. 1 Stress-strain curves of concrete in compression

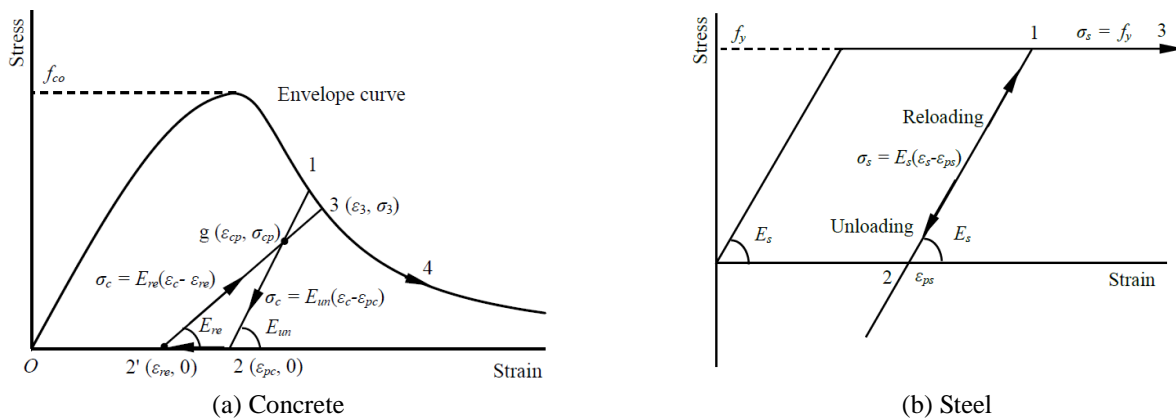(a) Concrete   (b) Steel

Fig. 2 Stress-strain relationship of constitutive materials with stress-path dependence

effect of confinement on the flexural ductility performance of both normal- and high-strength concrete beams is evaluated based on the rigorous full-range moment-curvature analysis with a view to developing empirical formulae and tables for the flexural ductility design of RC beams with confinement.

2. Nonlinear moment-curvature analysis

The deformability of RC beams with confinement is studied using the method of nonlinear moment-curvature analysis developed previously by the authors (Bai and Au 2013b) by employing the unified compression stress-strain curves for confined and unconfined concrete developed by Attard and Setunge (1996) and Attard and Stewart (1998), which have been shown to be applicable to a broad range of *in situ* concrete compressive strength f_{co} from 20 to 130MPa. The confining stress f_r is dependent on the volume ratio and yield strength of transverse reinforcement provided and can be evaluated using the method of Mander *et al.* (1988).

Fig. 1(a) shows some typical stress-strain curves of unconfined concrete with *in situ* concrete compressive strength f_{co} from 30 to 90MPa, while Fig. 1(b) shows those of confined concrete with *in situ* concrete compressive

strength f_{co} equal to 60MPa and confining stress f_r ranging from 0 to 2MPa. The model proposed by Elmorsi *et al.* (1998) as shown in Fig. 2(a) is adopted for concrete experiencing unloading and reloading. The elastic-plastic bilinear model is employed for steel as show in Fig. 2(b).

The moment-curvature curve of the beam section is analysed by applying the curvatures ϕ incrementally starting from zero. At a prescribed curvature ϕ, the stresses developed in the concrete and steel are determined form their stress-strain relationship taking into account loading path. Then, the neutral axis depth and resisting moment are evaluated form equilibrium conditions. Romberg integration (Gerald and Wheatley 1999) is used, which can significantly improve the accuracy of the simple trapezoidal rule when the integrand is known at equi-spaced intervals.

The above procedure is repeated until the resisting moment has increased to the peak and then dropped below 85% of the peak moment.

The beam sections analysed are rectangular in shape as shown in Fig. 3(a). A typical beam section has a breadth b = 300mm and total depth h = 600 mm, with the compression and tension reinforcement provided at depths d_1 = 60 mm and d = 540 mm from the top respectively, and with covers $c_1 = c_2 = c_3$ = 40 mm. The confining stress f_r is set to range from 0 to 2MPa to evaluate the confining effect. The steel yield strength f_y and Young's modulus E_s are assumed to be 400MPa and 200GPa respectively.
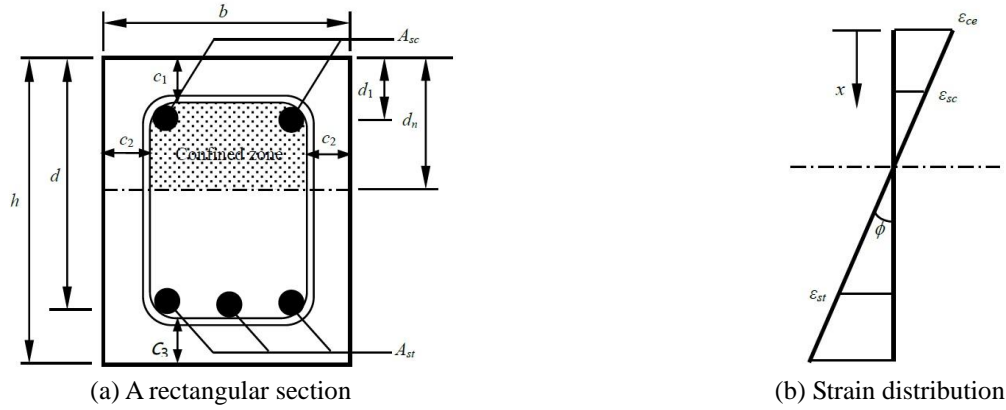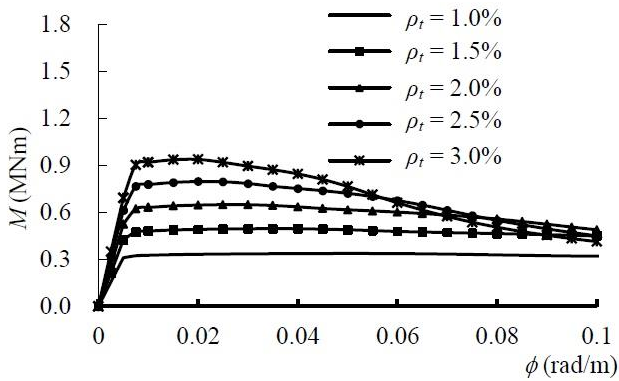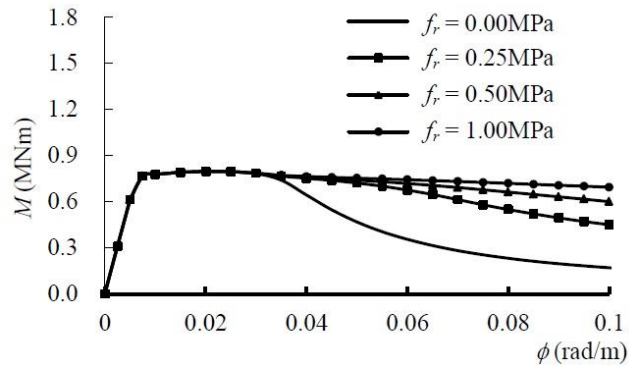
(a) A rectangular section   (b) Strain distribution

Fig. 3 A confined section subjected to bending moment

(a) f_r = 0.25MPa   (b) ρ_t = 2.5%

Fig. 4 Full-range moment-curvature curves of RC beam sections (f_{co} = 60MPa, ρ_c = 0.2%)

The *in situ* concrete compressive strength f_{co} ranges from 30 to 90MPa to cover both normal- and high-strength concrete. In accordance with the study of size effect by Bai (2006), a normalisation approach is adopted with dimensionless parameters so that the findings can be applied to cases of the same material properties and reinforcement arrangement but of different dimensions. According to Clause 9.2.1.1(3) of Eurocode 2 BSEN1992-1 (European Committee for Standardisation, 2004b), the compression steel ratio ρ_c = A_{sc}/bd studied varies from 0% to 4% to cover a relatively wide range. The tension steel ratio ρ_t = A_{st}/bd is always larger than the compression steel ratio. The present analysis has been extended to a reasonably high flexural ductility factor of 21 so as to cover more possibilities.
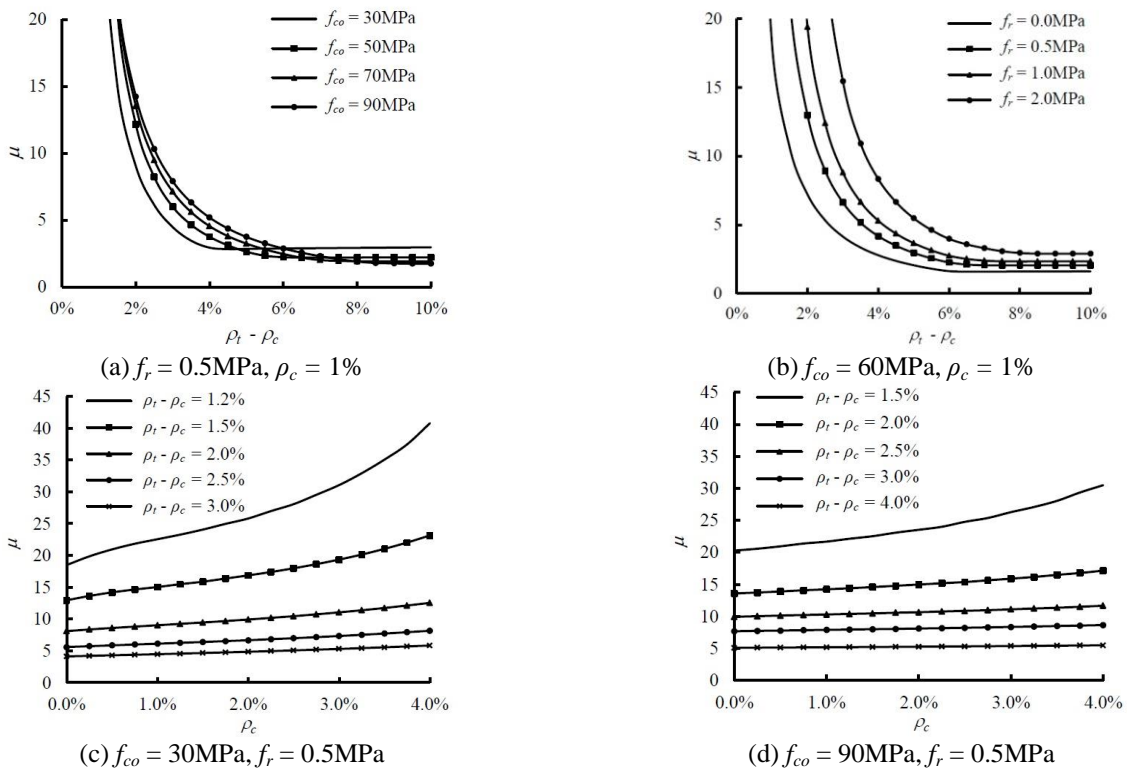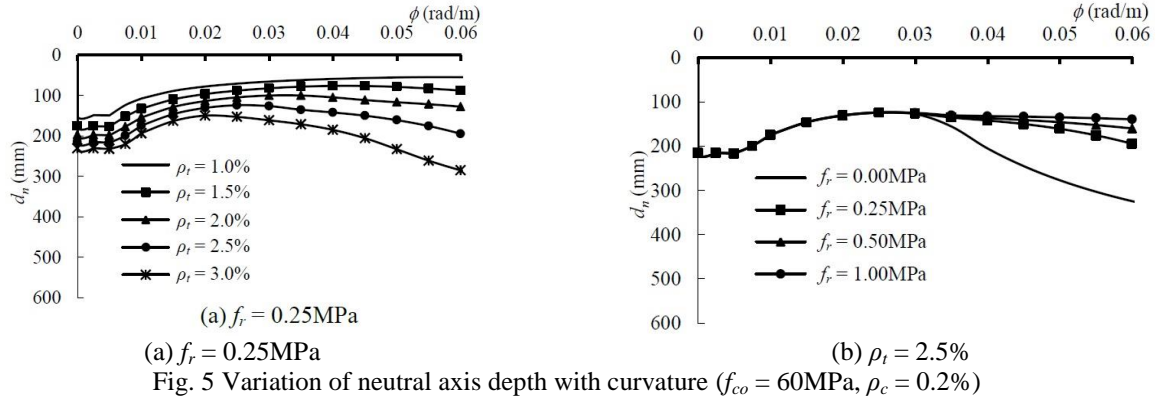
3. Results of analysis

3.1 Full-range moment-curvature curves

Fig. 4(a) shows some full-range moment-curvature curves of lightly confined RC beam sections with *in situ* concrete strength 60MPa at confining stress f_r = 0.25MPa. For the section with relatively low tension reinforcement ratio, the moment-curvature curve has lower stiffness at pre-peak stage, followed by a long plateau at post-peak stage. However, with increase in tension reinforcement ratio, the curve becomes sharper around the peak moment, indicating that the flexural ductility decreases with tension reinforcement ratio. When confinement is provided, the flexural strength of the section is hardly affected as shown in Fig. 4(b), but the peak tends to widen and the descending branch tends to have milder slope, clearly indicating improved flexural ductility with provision of confinement.

To better understand the full-range flexural behaviour, the variation of neutral axis depth d_n with curvature is illustrated in Fig. 5. As the curvature increases, the neutral axis depth remains constant initially and then gradually decreases when concrete becomes inelastic and the section enters the post-peak stage with unloading in part of compressive concrete. However, beyond a certain curvature at the post-peak stage, the neutral axis depth starts to increase again with curvature, thereby causing the neutral axis to approach the soffit and finally leading to reversal of strain and stress in tension reinforcement. Unlike the strain in tension reinforcement, the strain ε_{ce} at extreme concrete compression fibre and strain ε_{sc} in compression reinforcement always increase monotonically with curvature. With the increase of tension reinforcement ratio, the neutral axis depth is generally larger for the same curvature. This also leads to earlier reversal of strain and stress of tension reinforcement and more drastic decline of moment at the post-peak stage.

(a) $f_r = 0.25$MPa

(b) $\rho_t = 2.5\%$

Fig. 5 Variation of neutral axis depth with curvature ($f_{co} = 60$MPa, $\rho_c = 0.2\%$)

(a) $f_r = 0.5$MPa, $\rho_c = 1\%$

(b) $f_{co} = 60$MPa, $\rho_c = 1\%$

(c) $f_{co} = 30$MPa, $f_r = 0.5$MPa

(d) $f_{co} = 90$MPa, $f_r = 0.5$MPa

Fig. 6 Effects of structural parameters on curvature ductility factor μ

However, by providing more confinement, the neutral axis depth is reduced for the same curvature, which delays the reversal of strain and stress of tension reinforcement and hence reduces the rate of decline of moment at the post-peak stage.

3.2 Full-range moment-curvature curves

The curvature ductility factor μ of a beam section can be evaluated from the full-range moment-curvature curve in terms of the ultimate curvature φu and yield curvature φy as (Au and Kwan 2004, Bai *et al.* 2007, Bai and Au 2009, Bai and Au 2013b, Bai *et al.* 2015)

$$\mu = \phi_u / \phi_y \tag{1}$$

The ultimate curvature ϕ_u is defined as the curvature of the section when its moment has dropped to 85% of the peak moment after reaching the peak. The yield curvature ϕ_y is taken as that at the hypothetical yield point of an equivalent linearly elastic and perfectly plastic system with an elastic stiffness equal to the secant stiffness of the section at 75% of the peak moment and a yield moment equal to the peak moment. There are alternative ways for defining the ultimate curvature. For example, some design codes use the ultimate concrete strain in determining ultimate curvature (Baji *et al.* 2016). Depending on various parameters adopted, the outcome may or may not be more critical than the criterion used in this study.

Fig. 6 shows the effects of various structural parameters on the curvature ductility factor μ. The curvature ductility factor μ is plotted against the difference between tension

reinforcement ratio ρ_t and compression reinforcement ratio ρ_c in Figs. 6(a) and 6(b). When the tension reinforcement ratio ρ_t is relatively low and the tension reinforcement yields before the section reaches the peak moment, a ductile failure is produced, and the curvature ductility factor μ of a confined RC beam decreases with the increase of tension reinforcement ratio ρ_t when the compression reinforcement ratio ρ_c remains unchanged as shown in the left part of curves in Fig. 6(a). When the tension reinforcement ratio ρ_t is relatively high and the tension reinforcement remains elastic, a brittle failure is produced and the curvature ductility factor μ of a confined RC beam is virtually constant as shown in the right part of curves in Fig. 6(a). Fig. 6(a) also reflects the effect of concrete strength f_{co} on the curvature ductility factor μ of confined RC beam sections. Under the same reinforcement condition, the use of high-strength concrete increases the flexural ductility of RC beams in the ductile failure region. However, in the range corresponding to brittle failure, the residual constant curvature ductility factor μ of high-strength concrete is smaller than that of normal-strength concrete. On the other hand, Fig. 6(b) shows that confinement improves the flexural ductility of RC beams.

As increase in compression reinforcement tends to increase the flexural ductility, while increase in tension reinforcement tends to decrease it, it is useful to study the performance by varying the reinforcement ratios such that their difference $(\rho_t - \rho_c)$ remains unchanged. The variations of flexural ductility of confined RC beams of normal- and high-strength concrete are shown in Figs. 6(c) and 6(d) respectively. Except for those cases with relatively low value of difference in reinforcement ratios $(\rho_t - \rho_c)$, the effect of $(\rho_t - \rho_c)$ on flexural ductility is generally insignificant, particularly for high-strength concrete. When $(\rho_t - \rho_c)$ is small resulting in relatively high ductility, the curvature ductility factor μ is also more sensitive to the value of $(\rho_t - \rho_c)$, as shown in Fig. 6(c). However, at relatively high values of $(\rho_t - \rho_c)$ which result in relatively low ductility, such effect is negligible, particularly when high-strength concrete is used. Therefore the difference in reinforcement ratios $(\rho_t - \rho_c)$ can be regarded as the primary parameter that affects the flexural ductility of RC beams, while the common change of tension and compression reinforcement (i.e., ρ_c in Figs. 6(c) and 6(d)) as the secondary parameter only has limited effect on the flexural ductility of RC beams, as further elaborated below.

3.3 Flexural ductility design by limiting difference in reinforcement ratios

Limiting the difference in reinforcement ratios $(\rho_t - \rho_c)$ is an easy way to ensure the provision of a minimum curvature ductility factor μ_{min}. As the curvature ductility factor μ depends not only on the difference in reinforcement ratios $(\rho_t - \rho_c)$, but also on the concrete strength f_{co}, confining stress f_r and compression reinforcement ratio ρ_c, the value of maximum difference in reinforcement ratios $(\rho_t - \rho_c)$ allowed also varies with these parameters. In the present study, a trial and error approach has been adopted to evaluate the values of maximum difference in

reinforcement ratios $(\rho_t - \rho_c)$ allowed, which guarantees various practical minimum flexural ductility levels μ_{min} up to 21 with typical values of concrete strength f_{co}, confining stress f_r and compression reinforcement ratio ρ_c. The choice of 21 as the upper limit of μ_{min} allows the findings to be applied to structures of different ductility classes.
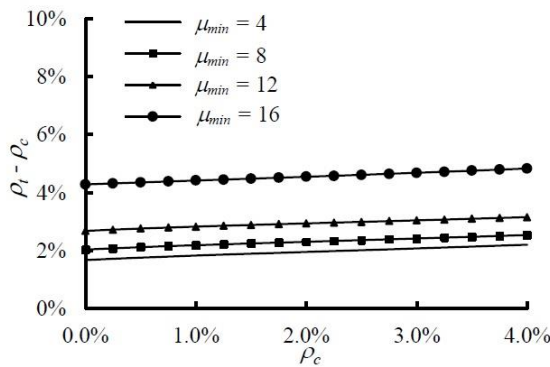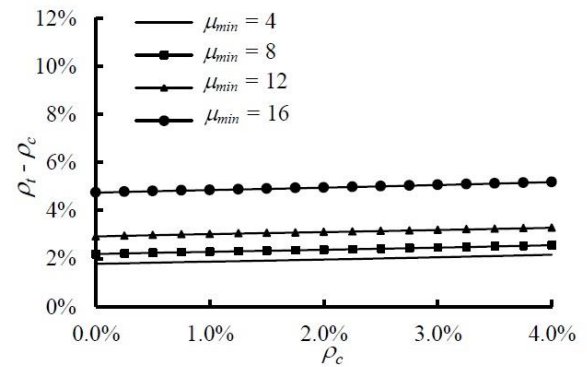
Fig. 7 shows the maximum values of difference in reinforcement ratios $(\rho_t - \rho_c)$ allowed plotted against the compression reinforcement ratio ρ_c for both normal- and high-strength concrete beams at a confining stress $f_r = 0.5\text{MPa}$. For a given set of concrete strength f_{co} and confining stress f_r, the value of maximum difference in reinforcement ratios $(\rho_t - \rho_c)$ allowed always decreases with increase in the minimum flexural ductility requirement. The effect of changes by the same amount in both compression and tension reinforcement on the maximum value of $(\rho_t - \rho_c)$ allowed is generally insignificant. It is only for the case of normal-strength concrete (i.e., $f_{co} = 30\text{MPa}$) and when the compression reinforcement ratio is very high (i.e., $\rho_c \geq 2.5\%$) that the increase of the same amount of both compression and tension reinforcement has some benefit on the maximum value of $(\rho_t - \rho_c)$ allowed. These findings are consistent with those of Bai and Au (2013b) for the flexural ductility design of high-strength concrete beams without confinement.

By regarding the changes by the same amount of both compression and tension reinforcement ratios as a secondary parameter that hardly affects the flexural ductility of RC beams, one may adopt a single value of $(\rho_t - \rho_c)_{max}$ that guarantees a minimum curvature ductility μ_{min} for a given set of concrete strength f_{co} and confining stress f_r.

The smallest values of maximum difference in reinforcement ratios $(\rho_t - \rho_c)_{max}$ within the range of compression reinforcement ratio studied and for a given set of concrete strength f_{co} and confining stress f_r are further evaluated. The typical results plotted against μ_{min} in Fig. 8 show that for a given set of concrete strength f_{co} and confining stress f_r, $(\rho_t - \rho_c)_{max}$ always decreases with increase in the minimum flexural ductility requirement. At relatively low confining stress, the value of $(\rho_t - \rho_c)_{max}$ significantly increases with concrete strength f_{co}. With increase of the confining stress, such enhancement in $(\rho_t - \rho_c)_{max}$ by using high-strength concrete decreases. Fig. 8 shows that for a given concrete strength f_{co} and minimum flexural ductility requirement μ_{min}, the value of $(\rho_t - \rho_c)_{max}$ increases with confining stress f_r.

Fig. 9 shows that the value of $(\rho_t - \rho_c)_{max}$ increases with the confining stress f_r and their relationship is largely linear. The general slope of the curve decreases as the concrete strength increases, which suggests that under the same confining stress, the increment in $(\rho_t - \rho_c)_{max}$ is more significant when the concrete strength is lower. This also explains the unusual observation at relatively high design level of minimum flexural ductility and relatively high confining stress in Fig. 8(d) that the value of $(\rho_t - \rho_c)_{max}$ tends to be similar for normal- and high-strength concrete.

To evaluate the maximum flexural strength M_p that can be achieved in flexural ductility design, the value of flexural strength ratio M_p/bd^2 is studied.
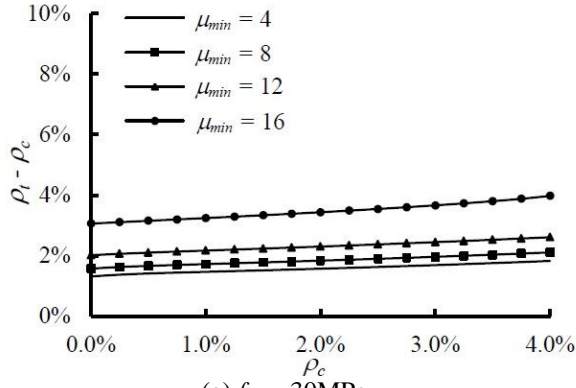
(a) $f_{co} = 30$MPa
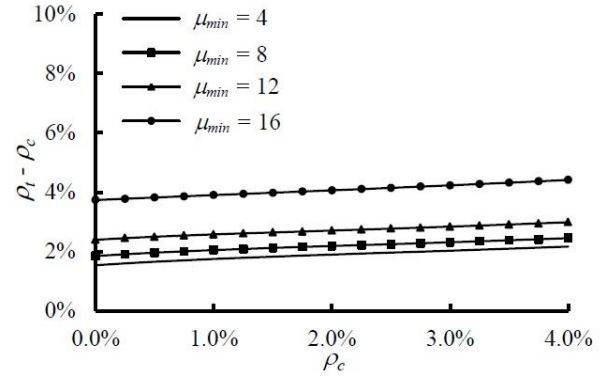
(b) $f_{co} = 50$MPa
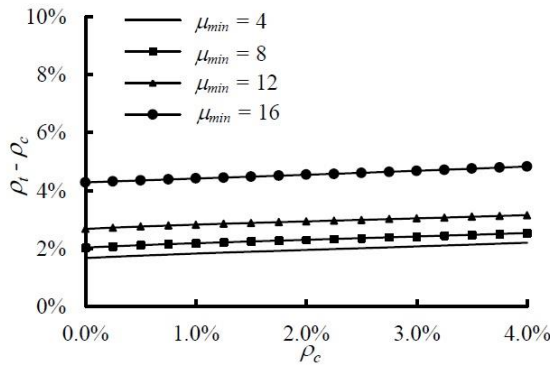
(c) $f_{co} = 70$MPa
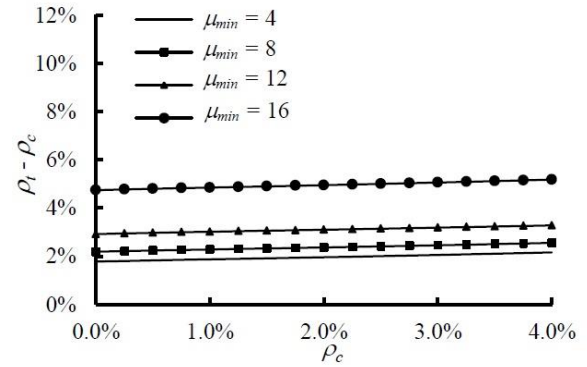
(d) $f_{co} = 90$MPa

Fig. 7 The maximum (ρ_t - ρ_c) with compression reinforcement ratio ρ_c ($f_r = 0.5$MPa)
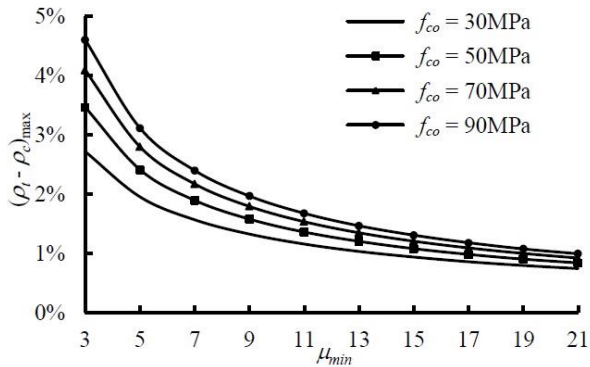
(a) $f_r = 0.0$MPa
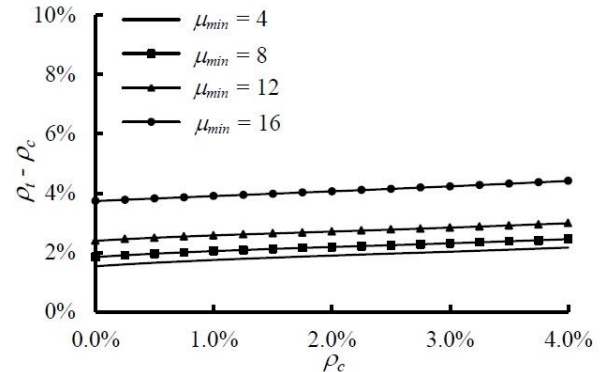
(b) $f_r = 0.5$MPa

(c) $f_r = 1.0$MPa

(d) $f_r = 2.0$MPa

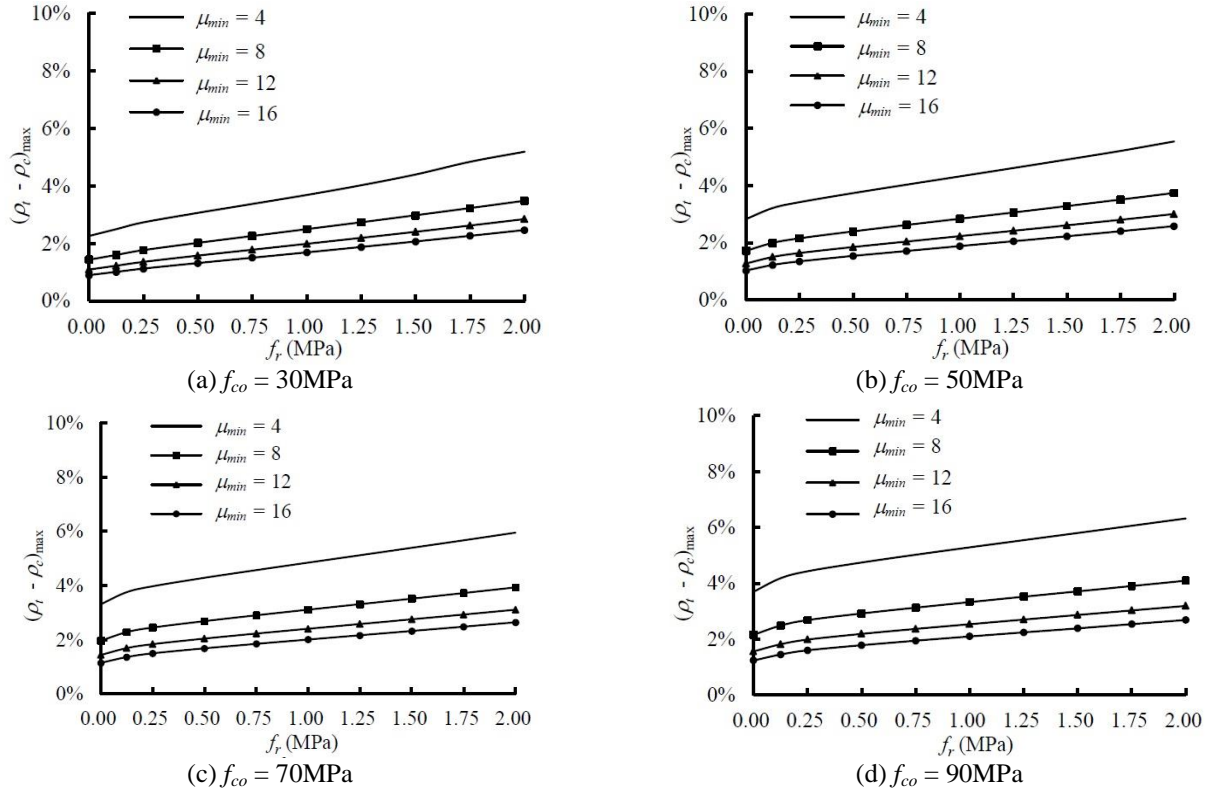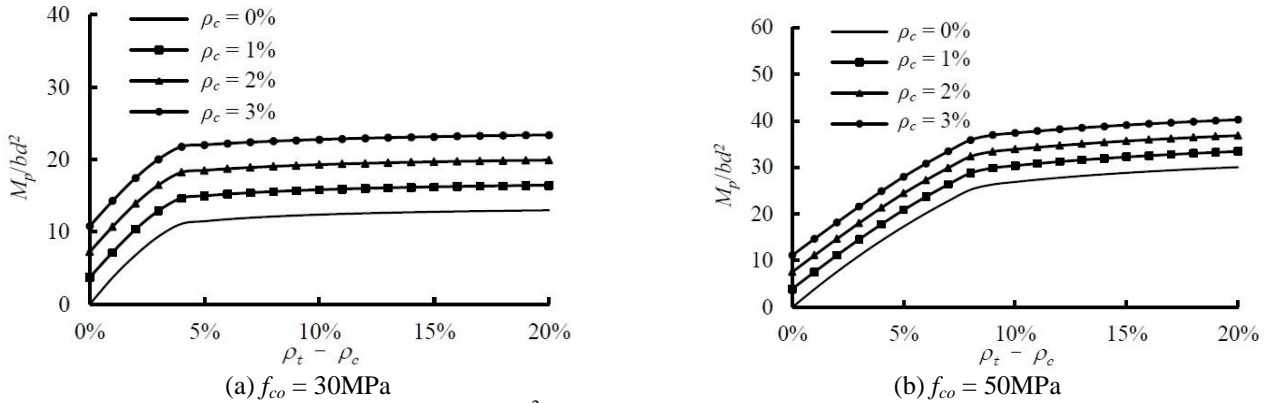Fig. 8 The value of (ρ_t - ρ_c)$_{max}$ with minimum flexural ductility μ_{min}

(a) f_{co} = 30MPa

(b) f_{co} = 50MPa

(c) f_{co} = 70MPa

(d) f_{co} = 90MPa

Fig. 9 Effect of confining stress on the value of $(\rho_t - \rho_c)_{max}$

(a) f_{co} = 30MPa

(b) f_{co} = 50MPa

Fig. 10 Normalised flexural strength M_p/bd^2 with difference in reinforcement ratios $(\rho_t - \rho_c)$ for f_r = 0.5MPa

Fig. 10 shows the relationship between flexural strength ratio M_p/bd^2 and difference in reinforcement ratios $(\rho_t - \rho_c)$ at confining stress f_r = 0.5MPa. For a given compression reinforcement ratio ρ_c and up to the balanced tension reinforcement ratio ρ_b, the flexural strength ratio M_p/bd^2 of a confined beam section increases with the value of $(\rho_t - \rho_c)$. However, beyond the balanced tension reinforcement ratio ρ_b, the RC beam section will fail in a brittle manner, and the increase in flexural strength ratio M_p/bd^2 is quite insignificant even when the amount of reinforcement increases significantly. Therefore for a given compression reinforcement ratio ρ_c, the maximum flexural strength ratio $(M_p/bd^2)_{max}$ of confined RC beams will be achieved practically when the maximum difference in reinforcement ratios $(\rho_t - \rho_c)_{max}$ is used.

To evaluate the effect of changes by the same amount of tension and compression reinforcement on the flexural strength ratio M_p/bd^2, one may study the value of M_p/bd^2, which denotes the increment in flexural strength ratio M_p/bd^2 of a doubly reinforced beam over that of the singly reinforced beam with the same value of $(\rho_t - \rho_c)$. Fig. 11 shows the relationship between increment of M_p/bd^2 and compression reinforcement ratio ρ_c. For a given value of $(\rho_c - \rho_c)$ = 3% and at confining stress f_r = 0.5MPa, the value of $\Delta M_p/bd^2$ is proportional to the value of ρ_c as shown in Fig. 11(a), while the value of $\Delta M_p/bd^2$ is virtually independent of the concrete strength.
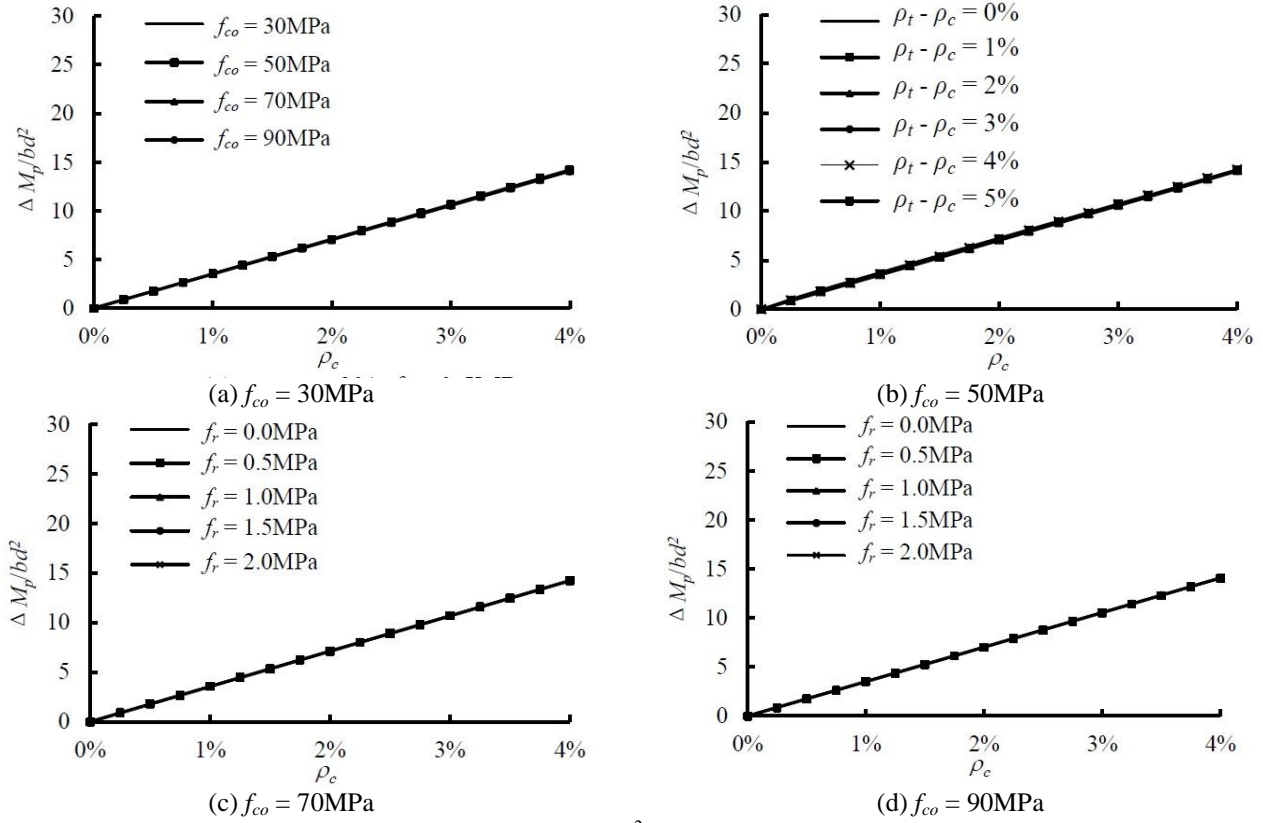
Fig. 11 Increment of normalized flexural strength $\Delta M_p/bd^2$ with changes by the same amount of compression and tension reinforcement
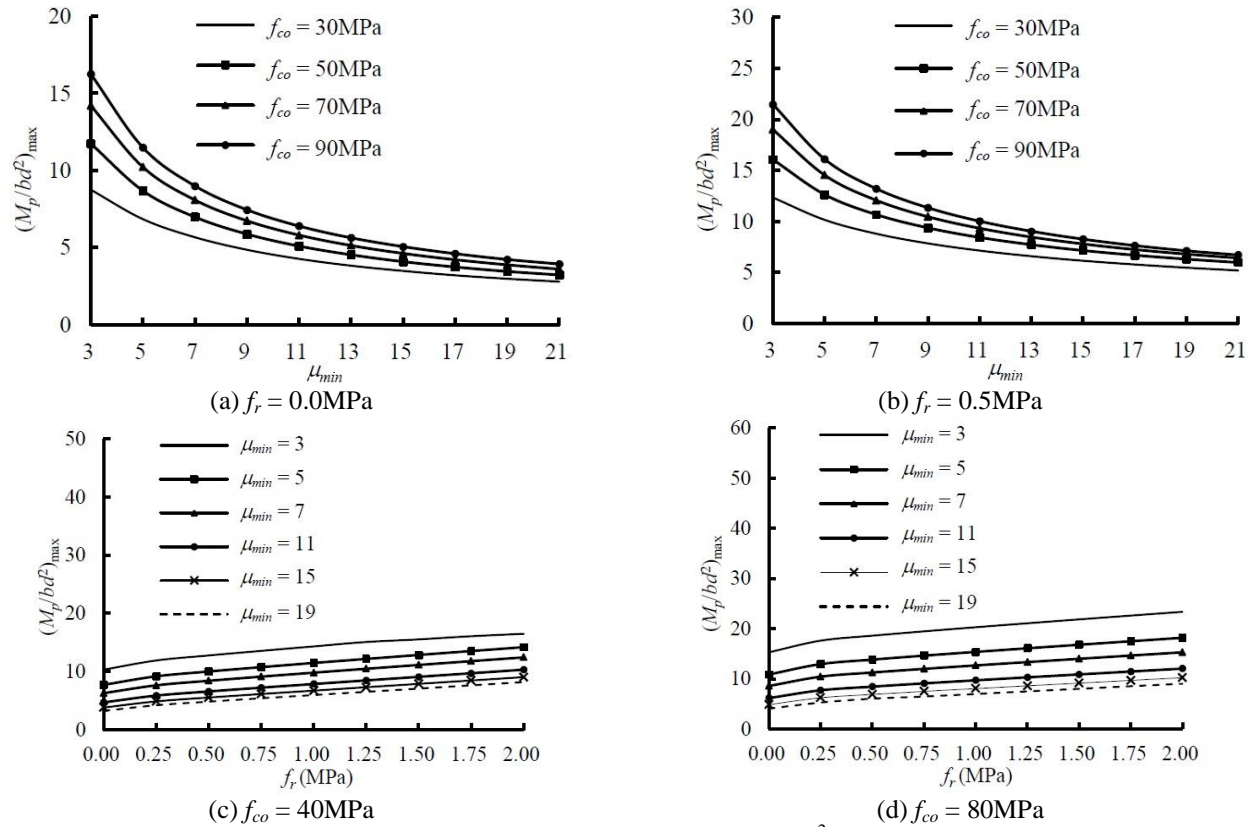

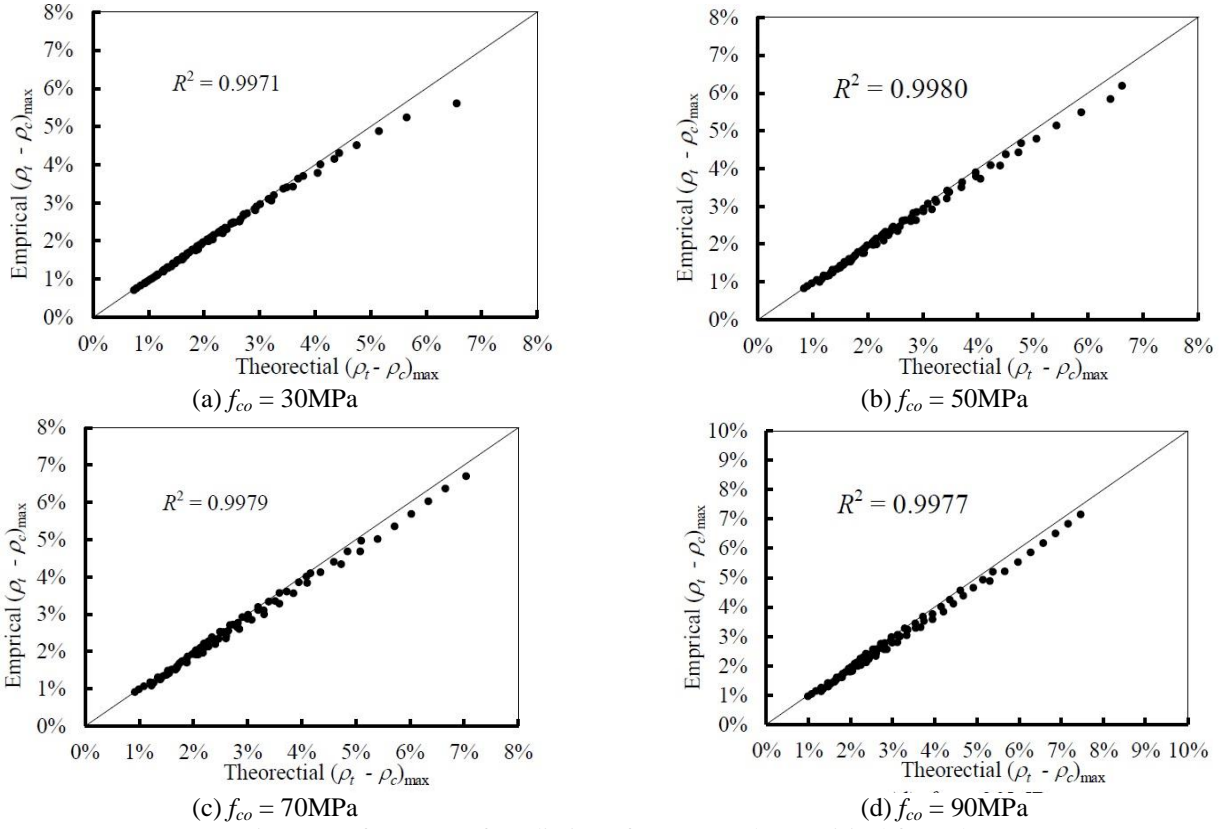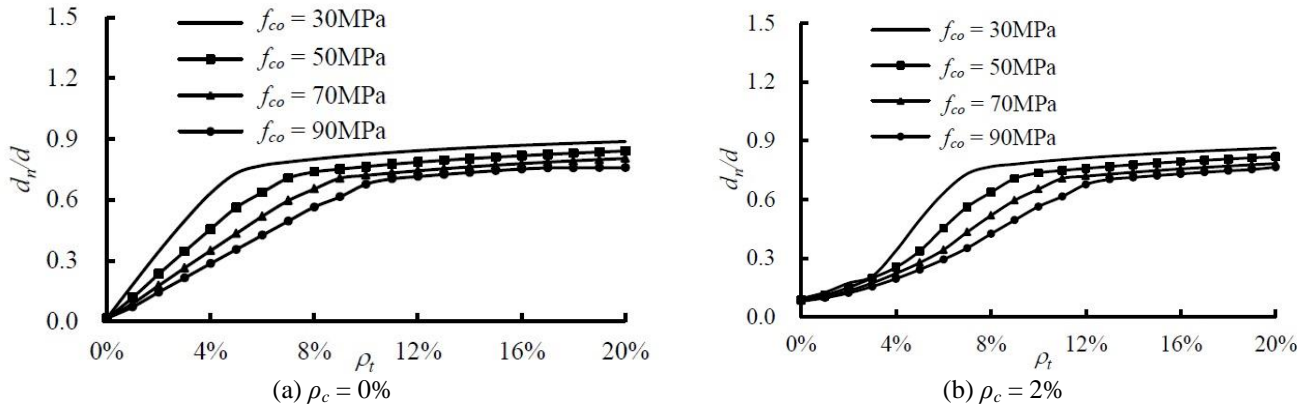Fig. 12 Variations of maximum normalized flexural strength $(M_p/bd^2)_{max}$ of singly reinforced beams

(a) $f_{co} = 30$MPa

(b) $f_{co} = 50$MPa

(c) $f_{co} = 70$MPa

(d) $f_{co} = 90$MPa

Fig. 13 Performance of prediction of $(\rho_t - \rho_c)_{max}$ by empirical formula

(a) $\rho_c = 0\%$

(b) $\rho_c = 2\%$

Fig. 14 Variation of neutral axis depth ratio d_n/d at peak resisting moment ($f_r = 0.5$MPa)

Fig. 11(b) shows that for a given concrete strength $f_{co} = 60$MPa at confining stress $f_r = 0.5$MPa, the value of $\Delta M_p/bd^2$ is also proportional to the value of ρ_c and virtually independent of the value of $(\rho_t - \rho_c)$. Figs. 11(c) and 11(d) further indicate that the value of $\Delta M_p/bd^2$ is also independent of the confining stress level. To sum up, observations show that the increment in flexural strength ratio M_p/bd^2 due to changes by the same amount of tension and compression reinforcement is proportional to the amount of the changes, but virtually independent of the concrete strength, initial reinforcement condition and confining stress.

As observed in Fig. 10, the maximum flexural strength ratio $(M_p/bd^2)_{max}$ of RC beams in the flexural ductility design can be reached when the maximum difference in reinforcement ratios $(\rho_t - \rho_c)_{max}$ is used. Since the increment in maximum flexural strength ratio $(M_p/bd^2)_{max}$ due to changes by the same amount of compression and tension reinforcement is the same for various concrete strength and confining stress, the maximum flexural strength ratio $(M_p/bd^2)_{max}$ of singly reinforced concrete beams can be employed to check whether and how much the use of high-strength concrete will benefit the flexural ductility with proper regard to flexural strength, as elaborated below.
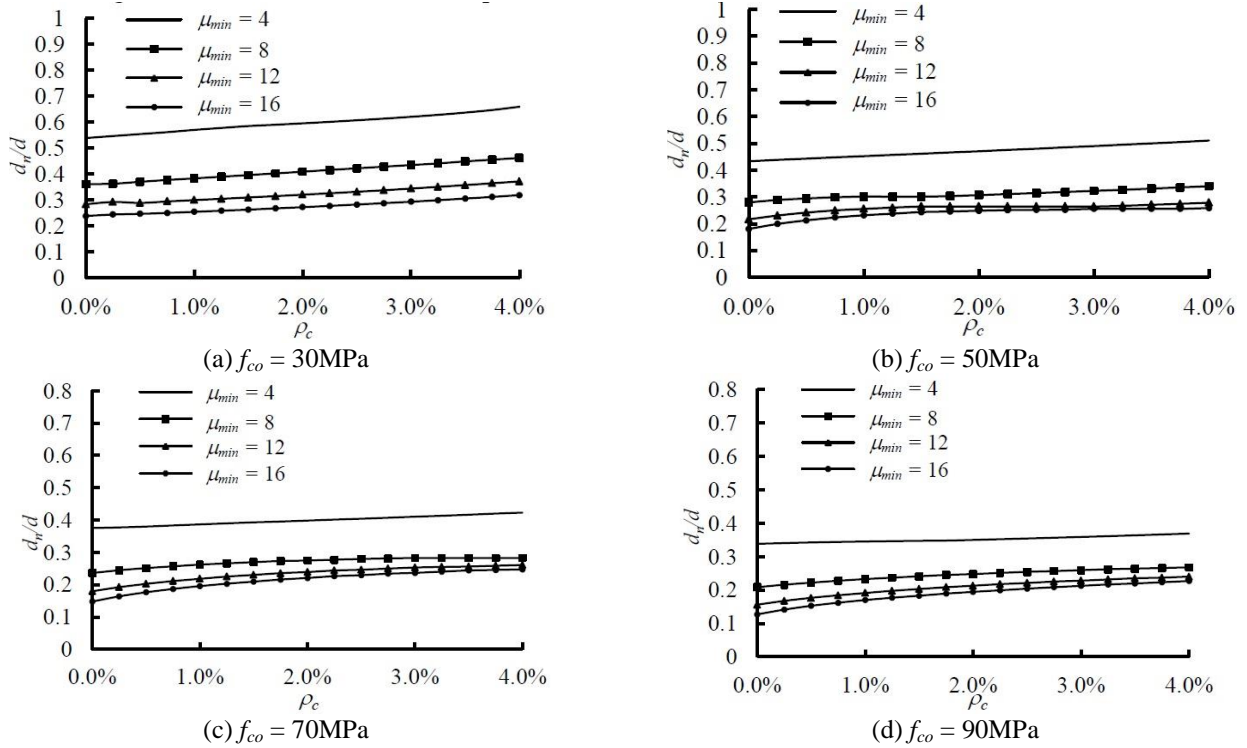
(a) $f_{co} = 30$MPa

(b) $f_{co} = 50$MPa

(c) $f_{co} = 70$MPa

(d) $f_{co} = 90$MPa

Fig. 15 Variation of maximum neutral axis depth ratio d_n/d with compression reinforcement ratio ρ_c ($f_r = 0.5$MPa)

Figs. 12(a) and 12(b) show the effects of concrete strength f_{co} and minimum flexural ductility level μ_{min} on the maximum normalised flexural strength $(M_p/bd^2)_{max}$ of singly reinforced beams.

As expected, the value of $(M_p/bd^2)_{max}$ always decreases with the increase in minimum flexural ductility requirement μ_{min}. Compared with the use of normal-strength concrete of $f_{co} = 30$MPa, the use of high-strength concrete can significantly enhance the values of maximum normalised flexural strength $(M_p/bd^2)_{max}$ as shown in Figs. 12(a) and 12(b) for both cases without and with confinement. Figs. 12(c) and 12(d) show that the maximum flexural strength ratio $(M_p/bd^2)_{max}$ achievable in the flexural ductility design increases significantly with confining stress for a given concrete strength.

In conclusion, the use of high-strength concrete can allow higher levels of both difference in reinforcement ratios and flexural strength to be achieved in the flexural ductility design of RC beams. The advantage of high-strength concrete is significant especially with relatively low design level of minimum flexural ductility, but the advantage gradually diminishes with the increase in design level of minimum flexural ductility. Moreover, the provision of confinement also increases both the difference in reinforcement ratios and flexural strength achievable.

Regression analysis of the numerical results gives an empirical formula for prediction of $(\rho_t - \rho_c)_{max}$ as

$$
\begin{aligned}
(\rho_t - \rho_c)_{max} = \\
10^{-4}(8.843 f_{co} + 305)\mu_{min}^{(20 f_{co} + 6207)/10^4} \\
+ 10^{-4} f_r (233.9 - 0.5 f_{co})\mu_{min}^{(5 f_{co} - 3883)/10^4}
\end{aligned} \tag{2}
$$

The comparison of empirical and theoretical values of $(\rho_t - \rho_c)_{max}$ in Fig. 13 shows excellent agreement with coefficients of correlation of R^2 above 0.99. Hence within the range of parameters studied, Eq. (2) is sufficiently accurate for practical applications.

3.4 Flexural ductility design by limiting neutral axis depth ratio

Fig. 14 shows the relationship between the neutral axis depth ratio d_n/d at peak resisting moment and the tension reinforcement ratio ρ_t at confining stress $f_r = 0.5$MPa. In general, for given compression reinforcement ratio ρ_c, concrete strength f_{co} and confining stress f_r, the neutral axis depth ratio d_n/d at peak resisting moment increases monotonically with the tension reinforcement ratio ρ_t. Hence for given compression reinforcement ratio ρ_c, concrete strength f_{co} and confining stress f_r of RC beams, the flexural ductility decreases with the increase of neutral axis depth ratio d_n/d at peak resisting moment. For theevaluated maximum differences in reinforcement ratios $(\rho_t - \rho_c)$ as shown in Fig. 7, the corresponding values of neutral axis depth ratio d_n/d at peak resisting moment can be determined from Fig. 15.

Limiting the neutral axis depth ratio d_n/d at peak resisting moment is another popular method in design codes for flexural ductility design of RC beams. Fig. 16 shows the maximum values of neutral axis depth ratio $(d_n/d)_{max}$ at peak resisting moment that guarantee various values of minimum flexural ductility factor μ_{min} throughout the range of compression reinforcement ratio studied. For given concrete strength f_{co} and confining stress f_r, $(d_n/d)_{max}$ always
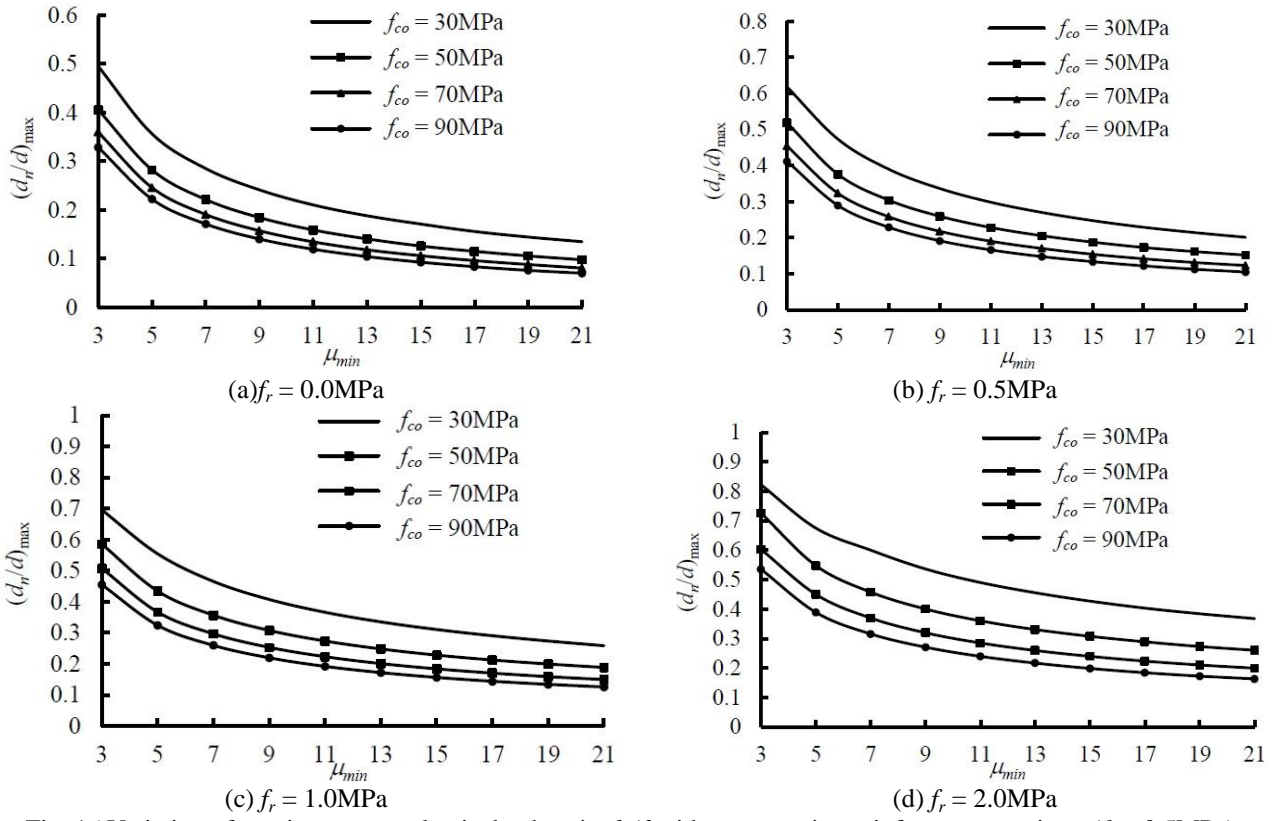
Fig. 16 Variation of maximum neutral axis depth ratio d_n/d with compression reinforcement ratio ρ_c ($f_r = 0.5$MPa)
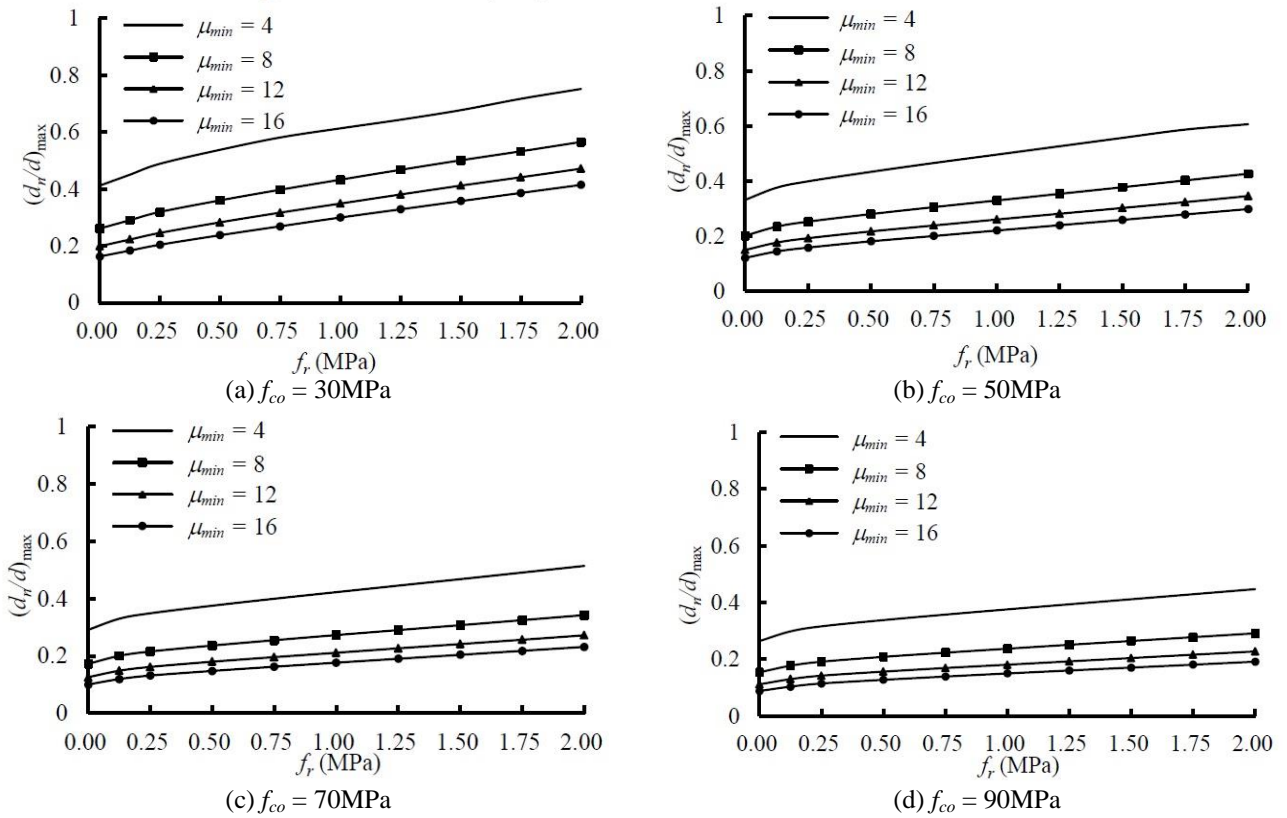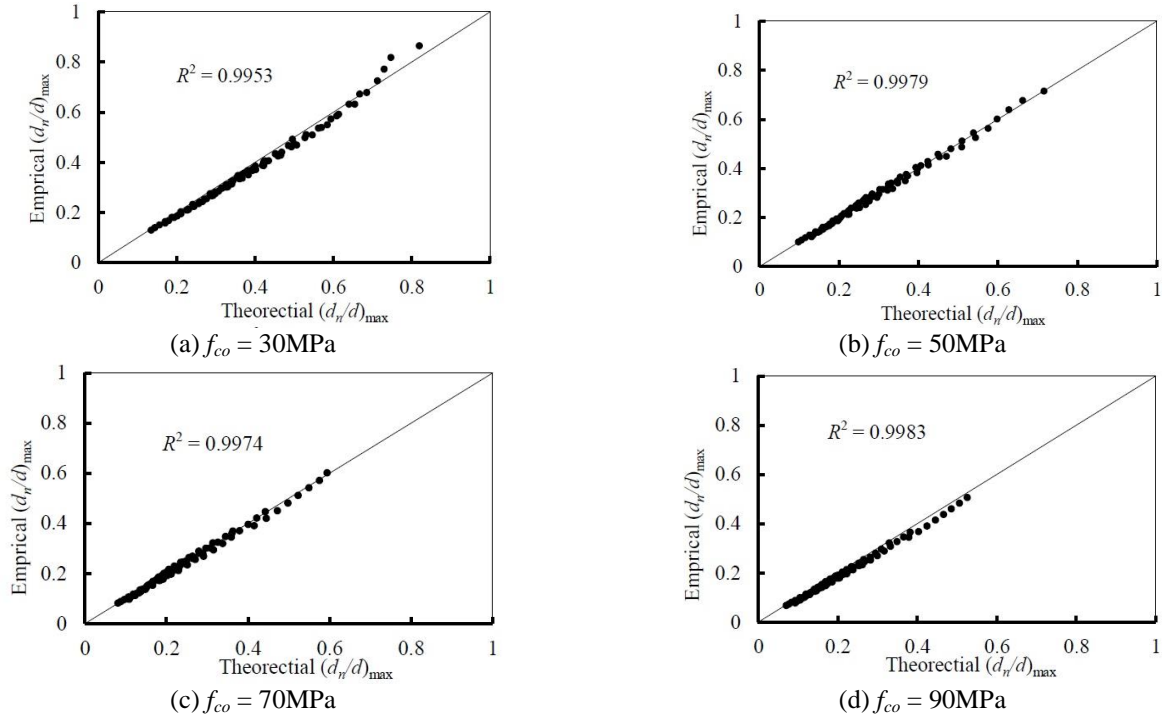

Fig. 17 Effect of confining stress on the value of $(d_n/d)_{max}$

(a) $f_{co} = 30$ MPa   (b) $f_{co} = 50$ MPa

(c) $f_{co} = 70$ MPa   (d) $f_{co} = 90$ MPa

Fig. 18 Performance of prediction of $(d_n/d)_{max}$ by empirical formula

Table 1 Basic value of behaviour factor q_o of concrete buildings that are regular in elevation according to Eurocode 8

Structural type	Sub-type	Basic value of	
		DCM	DCH
(a) Inverted pendulum system	—	1.5 (2.0)	2.0 (3.0)
(b) Torsionally flexible system	—	2.0 (3.0)	3.0 (5.0)
(c) Uncoupled wall system	(c-1) with only two uncoupled walls per	3.0 (5.0)	4.0 (7.0)
	(c-2) other uncoupled wall systems		4.4 (7.8)
(d) Frame system, dual system, and coupled-wall system	(d-1) One-storey frame	3.3 (5.6)	4.95 (8.9)
	(d-2) Multi-storey, one-bay frame	3.6 (6.2)	5.4 (9.8)
	(d-3) Multi-storey, multi-bay frame and	3.9 (6.8)	5.85 (10.7)

decreases with increase in μ_{min}. For given design level of flexural ductility μ_{min} and confining stress f_r, $(d_n/d)_{max}$ decreases significantly as the concrete strength f_{co} increases.

Fig. 17 confirms that, for given concrete strength and design level of flexural ductility, $(d_n/d)_{max}$ also increases roughly linearly with the confining stress f_r.

Regression analysis of the numerical results gives an empirical formula for prediction of $(d_n/d)_{max}$ as

$$
(d_n/d)_{max} = \\
2.562 f_{co}^{-0.2651} \mu_{min}^{-(20.33 f_{co}+6200)/10^4} \\
+ f_r (0.3031 - 0.0018 f_{co}) \mu_{min}^{-(0.2057+0.002 f_{co})} \tag{3}
$$

The comparison of empirical and theoretical values of $(d_n/d)_{max}$ in Fig. 18 shows excellent agreement with coefficients of correlation of R^2 above 0.99. Hence within the range of parameters studied, Eq. (3) is sufficiently accurate for practical applications.

3.5 Flexural ductility design to Eurocode

Earthquake resistant concrete buildings designed in accordance with Eurocode 8 BSEN1998-1 (European Committee for Standardisation, 2004a) are categorised by Clause 5.2.1(4) as ductility class DCM (medium ductility) or DCH (high ductility). Clause 5.2.2.1(1) of Eurocode 8 further classifies concrete buildings into various structural types according to their behaviour under horizontal seismic actions. With the basic value of behaviour factor q_o determined by the ductility class and structural type according to Clause 5.2.2.2, the minimum curvature ductility factor μ_{min} can then be determined by Clause 5.2.3.4(3) as

$$
\mu_{min} = 2q_o - 1 \quad \text{if} \quad T_1 \geq T_c \tag{4}
$$

Table 2 Maximum difference in reinforcement ratios $(\rho_t - \rho_c)_{max}$ according to Eurocode 8

Minimum ductility μ_{min}	Ductility Class / Structural Type for $T_1 \geq T_c$	$f_{ck,cube}$	C37	C50	C60	C75	C85	C95	C105
		f_{ck}	C30	C40	C50	C60	C70	C80	C90
		f_{co} (MPa)	27.0	36.0	45.0	54.0	63.0	72.0	81.0
		f_{cd} (MPa)	20.0	26.7	33.3	40.0	46.7	53.3	60.0
2.0	DCM (a)		3.41%	3.86%	4.30%	4.72%	5.14%	5.54%	5.94%
3.0	DCM (b)		2.59%	2.91%	3.22%	3.51%	3.80%	4.07%	4.32%
5.0	DCM (c-1)		1.84%	2.04%	2.24%	2.42%	2.59%	2.75%	2.90%
5.6	DCM (d-1)		1.70%	1.89%	2.07%	2.23%	2.38%	2.52%	2.65%
6.2	DCM (d-2)		1.59%	1.76%	1.92%	2.07%	2.21%	2.33%	2.45%
6.8	DCM (d-3)		1.49%	1.65%	1.80%	1.94%	2.06%	2.17%	2.28%
7.0	DCH (c-1)		1.46%	1.62%	1.76%	1.90%	2.02%	2.13%	2.23%
7.8	DCH (c-2)	$(\rho_t - \rho_c)_{max}$	1.36%	1.50%	1.63%	1.75%	1.86%	1.96%	2.05%
8.9	DCH (d-1)		1.24%	1.37%	1.49%	1.59%	1.69%	1.77%	1.85%
9.8	DCH (d-2)		1.17%	1.28%	1.39%	1.48%	1.57%	1.64%	1.71%
10.7	DCH (d-3)		1.10%	1.21%	1.30%	1.39%	1.47%	1.54%	1.60%
12.5			0.99%	1.08%	1.17%	1.24%	1.31%	1.36%	1.41%
15.0	Not		0.87%	0.96%	1.03%	1.09%	1.14%	1.19%	1.23%
18.0	applicable		0.77%	0.84%	0.90%	0.95%	1.00%	1.03%	1.06%
21.0			0.70%	0.76%	0.81%	0.85%	0.89%	0.92%	0.94%

Note: The increment in $(\rho_t - \rho_c)_{max}$ with 1MPa confining stress is shown in brackets

Table 3 Maximum normalised neutral axis depth $(d_n/d)_{max}$ according to Eurocode 8

Minimum ductility μ_{min}	Ductility Class / Structural Type for $T_1 \geq T_c$	$f_{ck,cube}$	C37	C50	C60	C75	C85	C95	C105
		f_{ck}	C30	C40	C50	C60	C70	C80	C90
		f_{co} (MPa)	27.0	36.0	45.0	54.0	63.0	72.0	81.0
		f_{cd} (MPa)	20.0	26.7	33.3	40.0	46.7	53.3	60.0
2.0	DCM (a)		3.41%	3.86%	4.30%	4.72%	5.14%	5.54%	5.94%
3.0	DCM (b)		2.59%	2.91%	3.22%	3.51%	3.80%	4.07%	4.32%
5.0	DCM (c-1)		1.84%	2.04%	2.24%	2.42%	2.59%	2.75%	2.90%
5.6	DCM (d-1)		1.70%	1.89%	2.07%	2.23%	2.38%	2.52%	2.65%
6.2	DCM (d-2)		1.59%	1.76%	1.92%	2.07%	2.21%	2.33%	2.45%
6.8	DCM (d-3)		1.49%	1.65%	1.80%	1.94%	2.06%	2.17%	2.28%
7.0	DCH (c-1)		1.46%	1.62%	1.76%	1.90%	2.02%	2.13%	2.23%
7.8	DCH (c-2)	$(\rho_t - \rho_c)_{max}$	1.36%	1.50%	1.63%	1.75%	1.86%	1.96%	2.05%
8.9	DCH (d-1)		1.24%	1.37%	1.49%	1.59%	1.69%	1.77%	1.85%
9.8	DCH (d-2)		1.17%	1.28%	1.39%	1.48%	1.57%	1.64%	1.71%
10.7	DCH (d-3)		1.10%	1.21%	1.30%	1.39%	1.47%	1.54%	1.60%
12.5			0.99%	1.08%	1.17%	1.24%	1.31%	1.36%	1.41%
15.0	Not		0.87%	0.96%	1.03%	1.09%	1.14%	1.19%	1.23%
18.0	applicable		0.77%	0.84%	0.90%	0.95%	1.00%	1.03%	1.06%
21.0			0.70%	0.76%	0.81%	0.85%	0.89%	0.92%	0.94%

Note: The increment in $(d_n/d)_{max}$ with 1MPa confining stress is shown in brackets

$$\mu_{\min} = 1 + 2(q_o - 1)\, T_c / T_1 \ \text{ if } \ T_1 < T_c \qquad (5)$$

where T_1 is the fundamental period of building and T_c is the period at the upper limit of the constant acceleration region of spectrum. If T_1 is not less than T_c, the minimum curvature ductility factor μ_{min} depends on q_o only; otherwise Eq. (5) implies that the minimum curvature ductility factor μ_{min} may increase and become very high as T_1 decreases.

According to Clause 5.2.2.2 of Eurocode 8, the basic values of behaviour factor q_o for ductility classes DCM and DCH for each structural type can be worked out. The structural types defined in Eurocode 8 are summarised in groups with ascending values of behaviour factor q_o as shown in Table 1, namely (a) inverted pendulum system; (b) torsionally flexible system; (c) uncoupled wall system; and (d) frame system, dual system, and coupled-wall system. Structural types (c) and (d) are further divided into several sub-types. The values of q_o in Table 1 are for concrete buildings that are regular in elevation. The reduction allowed for concrete buildings with irregular elevation is not considered. The corresponding minimum curvature ductility factors μ_{min} for concrete buildings with $T_1 \geq T_c$ are shown in brackets in Table 1.

Concrete structures designed in accordance with Eurocode 8 shall also comply with Eurocode 2 BS EN1992-1-1 (European Committee for Standardisation 2004b), which uses both the cylinder strength f_{ck} and the cube strength $f_{ck,cube}$ to define the concrete grade. Some correlation with the *in situ* concrete compressive strength f_{co} is therefore necessary in order to apply the present findings. The test results of Ibrahim and MacGregor (1996) show that the f_{co}/f_{ck} ratios of eccentrically loaded specimens range from 0.8 to 1.2 with an average value of 0.95, while those of concentrically loaded specimens vary between 0.7 to 1.1 with an average value of 0.85. For simplicity, a constant value of f_{co}/f_{ck} of 0.9 is adopted here.

Values of the maximum difference in reinforcement ratios $(\rho_t - \rho_c)_{max}$ without confinement are worked out for various minimum curvature ductility factors μ_{min} up to 21 and tabulated in Table 2. The increments in $(\rho_t - \rho_c)_{max}$ due to increment of 1MPa confining stress are also obtained as shown in brackets in Table 2. The minimum curvature ductility factors μ_{min} cover the structural types considered before for concrete buildings with $T_1 \geq T_c$. Similarly, values of $(d_n/d)_{max}$ at typical levels of minimum flexural ductility without confinement and the increment in $(d_n/d)_{max}$ due to increment of 1MPa confining stress are shown in Table 3.

4. Conclusions

The favourable effect of confinement on the flexural ductility of RC beams has been identified in this study. The difference in reinforcement ratios has been found to be the primary factor for flexural ductility design of confined RC beams, while changes by the same amount of tension and compression reinforcement hardly affect the flexural ductility and hence they can be ignored. A simple strategy has been developed for flexural ductility design of RC beams with confinement, together with empirical formulae and tables for application.

References

ACI Committee 318 (2014), *Building Code Requirements for Structural Concrete*, ACI 318-14 and Commentary, American Concrete Institute, Farmington Hills, U.S.A.

ACI Committee 363 (1992), *State-of-the-Art, Report on High Strength Concrete*, ACI 363-R92, American Concrete Institute, Detroit, Michigan, U.S.A.

Attard, M.M. and Setunge, S. (1996), "The stress-strain relationship of confined and unconfined concrete", *ACI Mater. J.*, **93**(5), 432-442.

Attard, M.M. and Stewart, M.G. (1998), "A two parameter stress block for high-strength concrete", *ACI Struct. J.*, **93**(5), 432-442.

Au, F.T.K. and Bai, Z.Z. (2006), "Effect of axial load on flexural behaviour of cyclically loaded RC columns", *Comput. Concrete*, **3**(4), 261-284.

Au, F.T.K. and Kwan, A.K.H. (2004), "A minimum ductility design method for non-rectangular high-strength concrete beams", *Comput. Concrete*, **1**(2), 115-130.

Bai, Z.Z., Au, F.T.K. and Chen, X.C. (2015), "Effect of small axial force on flexural ductility design of high-strength concrete beams", *Struct. Des. Tall Spec.*, **24**(11), 739-756.

Bai, Z.Z. (2006), "Nonlinear analysis of reinforced concrete beams and columns with special reference to full-range and cyclic behaviour", Ph.D. Dissertation, The University of Hong Kong, Hong Kong.

Bai, Z.Z. and Au, F.T.K. (2009), "Ductility of symmetrically reinforced concrete columns", *Mag. Concrete Res.*, **61**(5), 345-357.

Bai, Z.Z. and Au, F.T.K. (2013a), "Flexural ductility design of high-strength concrete columns", *Struct. Des. Tall Spec.*, **22**(1), 92-115.

Bai, Z.Z. and Au, F.T.K. (2013b), "Flexural ductility design of high-strength concrete beams", *Struct. Des. Tall Spec.*, **22**(6), 521-542.

Bai, Z.Z., Au, F.T.K. and Kwan, A.K.H. (2007), "Complete nonlinear response of reinforced concrete beams under cyclic loading", *Struct. Des. Tall Spec.*, **6**(2), 107-130.

Baji, H. and Ronagh, H.R. (2014), "A probabilistic study on the ductility of reinforced concrete sections", *Adv. Struct. Eng.* **17**(9), 1315-1327.

Baji, H., Ronagh, H.R. and Melchers, R.E. (2016), "Reliability of ductility requirements in concrete design codes", *Struct. Saf.*, **62**, 76-87.

Chen, M.T. and Ho, J.C.M. (2015), "Combined strain gradient and concrete strength effects on flexural strength and ductility design of RC columns", *Comput. Concrete*, **15**(4), 607-642.

Chen, X.C., Au, F.T.K., Bai, Z.Z., Li, Z.H. and Jiang, R.J. (2015), "Flexural ductility of reinforced and prestressed concrete sections with corrugated steel webs", *Comput. Concrete*, **16**(4), 625-642.

Elmorsi, M., Kianoush, M.R. and Tso, W.K. (1998), "Nonlinear analysis of cyclically loaded reinforced concrete structures",

ACI Struct. J., **95**(6), 725-739.

European Committee for Standardisation (2004a), *Eurocode 8: Design of Structures for Eearthquake Resistance-Part 1: General Rules, Seismic Actions and Rules for Buildings*, Brussels, Belgium.

European Committee for Standardisation (2004b), *Eurocode 2: Design of Concrete Structures-Part 1: General Rules and Rules for Building*, Brussels, Belgium.

Gerald, C.F. and Wheatley, P.O. (1999), *Applied Numerical Analysis*, 6th Edition, Addison-Wesley, U.S.A.

Ho, J.C.M., Au, F.T.K. and Kwan, A.K.H. (2005), "Effects of strain hardening of steel reinforcement on flexural strength and ductility of concrete beams", *Struct. Eng. Mech.*, **19**(2), 185-198.

Ibrahim, H.H.H. and MacGregor, J.G. (1996), "Flexural behavior of laterally reinforced high-strength concrete sections", *ACI Struct. J.*, **93**(6), 674-684.

Komleh, H.E. and Maghsoudi, A.A. (2015), "Prediction of curvature ductility factor for FRP strengthened RHSC beams using ANFIS and regression models", *Comput. Concrete*, **16**(3), 399-414.

Kwan, A.K.H. and Au, F.T.K. (2004), "Flexural strength-ductility performance of flanged beam sections cast of high-strength concrete", *Struct. Des. Tall Spec.*, **13**(1), 29-43.

Kwan, A.K.H., Au, F.T.K. and Chau, S.L. (2004), "Effects of confinement on flexural strength and ductility design of HS concrete beams", *Struct. Eng.*, **28**(23-24), 38-44.

Lee, H.J. (2013), "Predictions of curvature ductility factor of doubly reinforced concrete beams with high strength materials", *Comput. Concrete*, **12**(6), 831-850.

Mander, J.M., Priestley, N. and Park, R. (1998), "Theoretical stress-strain model for confined concrete", *J. Struct. Eng.*, **114**(8), 1804-1826.

Ministry of Construction of the People's Republic of China (2010), *Code for Seismic Design of Buildings*, GB50011-2010, Beijing, China.

Ministry of Construction of the People's Republic of China (2010), *Code for Seismic Design of Buildings*, GB50011-2010, Beijing, China.

Pam, H.J., Kwan, A.K.H. and Ho, J.C.M. (2001), "Post-peak behavior and flexural ductility of doubly reinforced normal- and high-strength concrete beams", *Struct. Eng. Mech.*, **12**(5), 459-474

Pandey, A.K. (2013), "Flexural ductility of RC beam sections at high strain rates", *Comput. Concrete*, **12**(4), 537-552.

Priastiwi, Y.A., Imran, I. and Hidayat, A. (2014), "Behavior of ductile beam with addition confinement in compression", *Proc. Eng.*, **95**, 132-138.

Ziara, M.M., Haldane, D. and Kuttab, A.S. (1995), "Flexural behavior of beams with confinement", *ACI Struct. J.*, **92**(1), 103-114.

CC